

# Neutron skin impurity from Coulomb core-polarization in $^{208}\text{Pb}$ : Insights from PREX-II and validation via $(^3\text{He}, t)$ IAS reaction

Phan Nhut Huan\*

*Institute of Fundamental and Applied Sciences, Duy Tan University, Ho Chi Minh City 70000, Vietnam and  
Faculty of Natural Sciences, Duy Tan University, Da Nang City 50000, Vietnam*

(Dated: May 30, 2024)

We investigate the impurity in the neutron skin induced by Coulomb core-polarization, highlighting its impact on uncertainties in neutron skin measurements from PREX-II. This effect is validated using the  $(^3\text{He}, t)$ IAS reaction at 420 MeV. Our findings reveal that the Coulomb boundary radius, where core-polarization becomes negligible, is critical for accurately probing the neutron skin in the target nucleus. Notably, the  $(^3\text{He}, t)$ IAS experiment conducted by Zegers et al. [Phys. Rev. Lett. 99, 202501 (2007)] primarily detects neutron excess at zero scattering angle due to the core-polarization phenomenon, rather than the neutron skin. We propose extending this experiment to measure cross sections at a  $3^\circ$  angle to more precisely determine the neutron skin thickness in  $^{208}\text{Pb}$ . Additionally, uncertainties in PREX-II may arise from electrons initially probing neutron excess instead of the neutron skin, potentially leading to an overestimation of neutron skin thickness due to the mixing effect where protons are displaced into the neutron skin region.

Comprehending nucleon distribution within atomic nuclei is essential for advancing nuclear physics, exploring the equation of state (EOS) of neutron-rich matter, and addressing astrophysical phenomena [1]. Accurate proton and neutron distributions are vital, with neutron skin thickness in heavy nuclei offering insights into neutron star properties [2]. Probing these distributions is challenging due to differing techniques for protons and neutrons. Protons are measured using electron scattering, providing charge density distributions crucial for nuclear structure studies. In contrast, neutron distributions are evaluated through proton-nucleus elastic scattering, such as in the RCNP experiment, which measured the neutron skin thickness in  $^{208}\text{Pb}$  as  $0.211_{-0.063}^{+0.054}$  fm [3]. Nevertheless, parity-violating electron scattering (PVES) in the Lead Radius Experiment (PREX) is the most promising model-independent technique. PREX-I [4] and PREX-II [5] at Jefferson Laboratory measure neutron distribution in  $^{208}\text{Pb}$  using PVES, leveraging the weak force's stronger coupling to neutrons. PREX-II results reveal a neutron skin thickness of  $\Delta R_{np} = 0.283 \pm 0.071$  fm. Furthermore, reanalysis of PREX-II using contemporary relativistic and non-relativistic energy density functionals (EDFs) predicts a neutron skin thickness of  $\Delta R_{np} = 0.19 \pm 0.02$  fm and a symmetry energy slope  $L = 54 \pm 8$  MeV, aligning with astrophysical observations and providing stringent constraints on nuclear models [6].

This study addresses significant uncertainties in neutron skin thickness measurements, particularly in the PREX-II experiment for  $^{208}\text{Pb}$ . A major contributor to these uncertainties is the often-overlooked effect of Coulomb core-polarization, which markedly impacts measurement accuracy. Auerbach and Van Giai [7] investigated the connection between neutron excess, isovector density, and Coulomb core-polarization, showing that the Coulomb force induces core polarization by displac-

ing protons outward, creating a density,  $\delta\rho$ , with positive values inside the nucleus and negative values outside, forming a nodal structure. This effect is pronounced when  $\rho_{nexc}$  is small, especially in nuclei with a significant Coulomb potential. In  $^{208}\text{Pb}$ , the core-polarization is considerable due to the large proton number, despite the substantial neutron excess, leading to uncertainties in neutron skin thickness measurements. In PREX-II, incident particles primarily interact with the neutron excess rather than the neutron skin, potentially causing inaccuracies in determining the neutron distribution. Therefore, these uncertainties may be attributed to core-polarization effects, notating the need to account for this phenomenon in interpreting experimental data.

The  $(^3\text{He}, t)$  charge-exchange reaction is commonly utilized to investigate the spin-isospin properties of nuclei [8]. This reaction has been effectively employed to discover neutron skin thickness, particularly through Fermi transitions between the isobaric analog state (IAS) and the target ground state. Loc et al. [9] demonstrated this application by utilizing the IAS peak at zero scattering angle, and theoretical models provided an optimal distorted wave Born approximation (DWBA) fit for the experimental data from Zegers et al. [8], enabling the determination of neutron skin thickness in  $^{208}\text{Pb}$ . The reliability of this method was further corroborated microscopically by Huan et al. [10] using the  $G$ -matrix double folding model, which deduced a neutron skin thickness of  $\Delta R_{np} = 0.16$  fm. The sensitivity of the  $(^3\text{He}, t)$ IAS reaction to the isovector term of the optical potential, which depends on the neutron-proton density difference, underlines its utility in assessing neutron skin thickness.

At zero scattering angle, the  $(^3\text{He}, t)$ IAS reaction may primarily probe neutron excess rather than neutron skin due to the core-polarization phenomenon, as discussed by Auerbach et al. [7] and Loc et al. [11]. In nuclei with a

small neutron excess, using neutron excess as the transition density instead of isovector density results in better experimental agreement, as the incident particle interacts with a denser neutron region. In  $^{208}\text{Pb}$ , the 82 protons amplify the core-polarization influence, displacing protons toward the nucleus's surface and potentially affecting experiments like PREX-II, where electrons might probe neutron excess instead of neutron skin. Recognizing the core-polarization as an intrinsic property is critical. The inconsistency between the neutron skin thickness  $\Delta R_{np} = 0.16$  fm found by Huan et al. [10] and the recent PREX-II result  $\Delta R_{np} = 0.283 \pm 0.071$  fm [5] suggests that the  $(^3\text{He}, t)$ IAS reaction at zero scattering angle may observe neutron excess rather than neutron skin. This illuminates the importance of accounting for the core-polarization behavior and indicates that measurements at non-zero scattering angles may be necessary for precisely determining neutron skin thickness.

To investigate the core-polarization impact, we utilize a double-folding model [9, 10] incorporating Chiral three-nucleon forces (3NFs)  $G$ -matrix interaction [12], providing a fully microscopic description of the  $(^3\text{He}, t)$ IAS reaction without adjusting any free parameters. Additionally, the densities of the  $^3\text{He}$  and triton particles are derived from a three-body calculation using the Argonne v18 interaction [13]. Target nuclear densities are obtained from Skyrme Hartree-Fock calculations [14] using the SAMi-J EDF family [15]. The SAMi interaction, recognized for its improved spin-isospin properties, is specifically fitted to the properties of  $^{208}\text{Pb}$  [16], ensuring a consistent mean-field description. As summarized in Table I, these variants allow us to explore different neutron skin thickness values in  $^{208}\text{Pb}$ , consistent with RCNP, PREX-II, and reanalyzed PREX-II results. By varying the symmetry energy, we cover a wide range of neutron skin thickness values, providing a comprehensive basis for assessing the core-polarization process. Our double-folding model, integrated with Chiral 3NFs  $G$ -matrix and SAMi-derived densities, offers a fully microscopic framework ideally compatible with this analysis.

TABLE I. Properties of the  $^{208}\text{Pb}$  from Skyrme Hartree-Fock calculations using the SAMi-J interaction. Neutron skin thickness  $\Delta R_{np}$  and  $\Delta R_{core} = R_{ncore} - R_{pcore}$ , reflecting the Coulomb core-polarization, are listed for different SAMi-J interactions. All root mean square (rms) values are in fm.

Skyrme int.	$R_n$	$R_p$	$\Delta R_{np}$	$R_{ncore}$	$R_{pcore}$	$\Delta R_{core}$	$R_{nexc}$
SAMi-J29	5.625	5.463	0.162	5.321	5.463	-0.142	6.150
SAMi-J30	5.647	5.467	0.180	5.344	5.467	-0.123	6.173
SAMi-J31	5.668	5.469	0.199	5.366	5.469	-0.103	6.193
SAMi-J35	5.728	5.462	0.266	5.428	5.462	-0.034	6.249

To validate the core-polarization behavior, we demonstrate that the  $(^3\text{He}, t)$ IAS reaction probes neutron excess rather than neutron skin at forward scattering an-

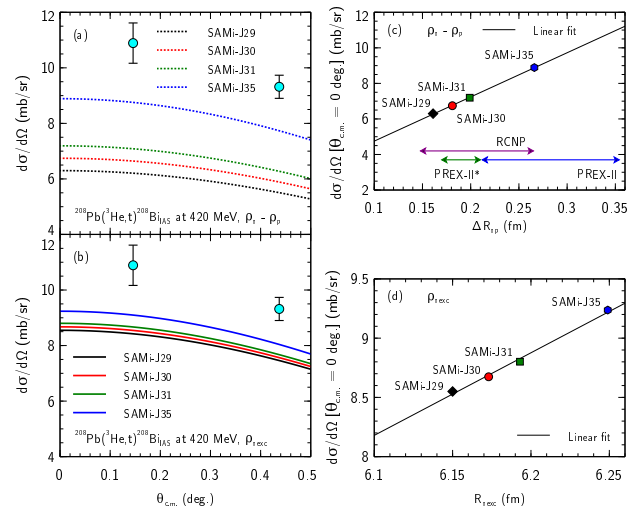


FIG. 1. Differential cross section results of the  $(^3\text{He}, t)$ IAS reaction at forward angles with SAMi-J interactions, using (a) isovector density, and (b) neutron excess density. Correlation between the differential cross section at zero scattering angle versus (c) neutron skin thickness using isovector density, and (d) rms radius of neutron excess distribution using neutron excess density. Experimental data are from Zegers et al. [8]. These results emphasize the sensitivity of the  $(^3\text{He}, t)$ IAS reaction to neutron excess at zero scattering angle due to the Coulomb core-polarization influence. PREX-II\* refers to the reanalyzed results of PREX-II [6].

gles from  $0^\circ$  to  $0.5^\circ$ . This is particularly relevant at zero scattering angle, where the IAS peak is observed and typically used to probe neutron skin, as noted by Loc et al. [9] and Huan et al. [10]. Our findings point out that at these angles, the  $(^3\text{He}, t)$ IAS reaction primarily probes neutron excess. This is illustrated in Fig. 1, showing the differential cross section at forward angles from  $0^\circ$  to  $0.5^\circ$  using a linear scale. We consider two options for transition density: conventional isovector density [Fig. 1(a)] and neutron excess density [Fig. 1(b)]. As the neutron skin increases from SAMi-J29 to SAMi-J35, the differential cross section at forward angles is enhanced with both densities, more so with neutron excess density due to higher density encountered by the incident  $^3\text{He}$  particle. This enhancement is attributed to the core-polarization process, which pushes protons outward, creating a inconsistency between neutron excess and neutron skin at the surface. Figure 1(c) shows the correspondence between neutron skin and differential cross section at zero scattering angle using isovector density, demonstrating a linear association. Conversely, Figure 1(d) illustrates the connection between differential cross section at zero scattering angle using neutron excess density versus the rms radius of the neutron excess distribution, showing a similar linear trend. The differential cross section increases with larger neutron excess, indicating that Skyrme interactions predicting increased neu-

tron skin also show larger rms values for neutron excess distribution at the surface (see Table I). This proves that the  $(^3\text{He}, t)$ IAS reaction, more sensitive to neutron excess at zero scattering angle due to the core-polarization phenomenon, probes the neutron excess rather than the neutron skin at the surface, underscoring the necessity of validating this effect. This explains the discrepancy in neutron skin values observed in previous studies, such as the  $\Delta R_{np} = 0.16$  fm reported by Huan et al. [10], compared to the  $\Delta R_{np} = 0.283 \pm 0.071$  fm result from PREX-II.

We further elucidate the underlying physics from both nuclear structure and nuclear reaction perspectives. Figures 2(a,d,g) display the nuclear distribution of  $^{208}\text{Pb}$  for SAMi-J29, SAMi-J31, and SAMi-J35, respectively, illuminating the isovector, neutron excess, and Coulomb core-polarization densities. A clear inconsistency between neutron excess and isovector density is observed at the nucleus surface, where protons are pushed toward, resulting in negative density in the surface region. When an incident particle probes the target (exhibited by a black horizontal arrow), it first encounters the neutron excess region, characterized by the rms of the neutron excess distribution. This interaction, as demonstrated in Fig. 1, occurs at zero scattering angle. Figures 2(b,c), 2(e,f), and 2(h,i) show the real and imaginary parts of the transition potential, which identify the differential cross section of the  $(^3\text{He}, t)$ IAS reaction, using isovector and neutron excess transition densities. The transition potential characterizes the reaction probability and directly influences the differential cross section. The concept of the Coulomb boundary radius, where protons begin to be displaced outward. As the incident particle probes this region, it first interacts with the neutron excess area, resulting in an enhanced transition potential when using neutron excess density. This consistent behavior in both real and imaginary parts, aligning with the isospin-dependent part in the Chiral 3NFs G-matrix, underscores the microscopic nature of our model, with significant contributions from imaginary coupling. The Coulomb boundary radius values are found to be 5.8 fm for SAMi-J29, 5.7 fm for SAMi-J31, and 5.4 fm for SAMi-J35. The same behavior in transition potential, including the point where the two transition potentials converge, is observed at a radius almost exactly equal to the Coulomb boundary radius. This demonstrates that the core-polarization significantly affects the determination of neutron skin thickness. At the boundary radius, the incident particle exactly probes the neutron skin as the core-polarization impact diminishes, resulting in similar transition potentials for both neutron excess and isovector densities, consistent in both real and imaginary parts.

In fundamental physics, neutron skin is created by the symmetry potential, arising naturally from the asymmetry between protons and neutrons, known as neutron excess. However, the Coulomb core-polarization phe-

nomenon, an intrinsic property, cannot be ignored. The similar strength of the transition potential at the convergence point denotes nearly the same reaction probability, as shown by the differential cross section. We identified a region where the differential cross section is the same for both transition potentials, specifically at the first minimum, approximately between  $1.8^\circ$  and  $2.1^\circ$ , as shown in the supplementary figure. This region reveals where the incident particle reaches the Coulomb boundary radius, reflected in the differential cross section as a function of angle. Considering the effect of core-polarization with increasing neutron skin values, validated by different SAMi interactions, we observe that the Coulomb boundary radius shifts from 5.8 fm to 5.4 fm as the neutron skin increases. The extent of protons driven outward due to core-polarization decreases with increasing neutron skin, as the symmetry potential becomes more dominant. This predominance is evident from the shifting Coulomb boundary radius and the reduction in  $\Delta R_{\text{core}}$ , which becomes less negative, as shown in Table I. The incompatibility between  $R_{\text{nexc}}$  and  $R_{\text{n}}$ , influenced by both the Coulomb and symmetry potentials, is greater than  $\Delta R_{\text{core}}$ , which is affected solely by the Coulomb interaction. This shift and reduction in proton displacement highlight the reduced effect of core-polarization with increasing neutron skin, as clearly seen in SAMi-J35, which has the highest neutron skin value of 0.266 fm, close to the PREX-II result. This reduced effect results in minimal divergences in the transition potentials and corresponding differential cross sections obtained with the two transition densities.

Examining Figures 2(a,d,g), we observe the density distribution in the target structure, with the neutron skin region displayed by the cyan transparent area. For SAMi-J29, with a neutron skin value of 0.162 fm, the incident particle first probes the neutron excess distribution, as indicated by the differential cross section at zero scattering angle discussed earlier. Then, the particle reaches the Coulomb boundary radius, where core-polarization is unnoticeable, corresponding to the cross section near the first minimum ( $1.8^\circ$  to  $2.1^\circ$ ). Here, the neutron skin region lies beyond the Coulomb boundary radius, meaning the particle naturally probes the neutron skin thickness in  $^{208}\text{Pb}$  beyond the first minimum. A similar trend is observed for SAMi-J31, with an increased neutron skin value of 0.199 fm. The Coulomb boundary radius shifts inward to 5.7 fm due to the dominant symmetry potential compared to the Coulomb effect. Thus, the scattering angle used to probe the neutron skin remains consistent with the SAMi-J29 case, occurring after the first minimum angle. In the case of SAMi-J35, with a neutron skin value of 0.266 fm, nearly matching the PREX-II result, an intriguing behavior is observed. The high neutron skin value demonstrates a predominant symmetry potential, shifting the Coulomb boundary radius further inward. Interestingly, the Coulomb boundary radius now

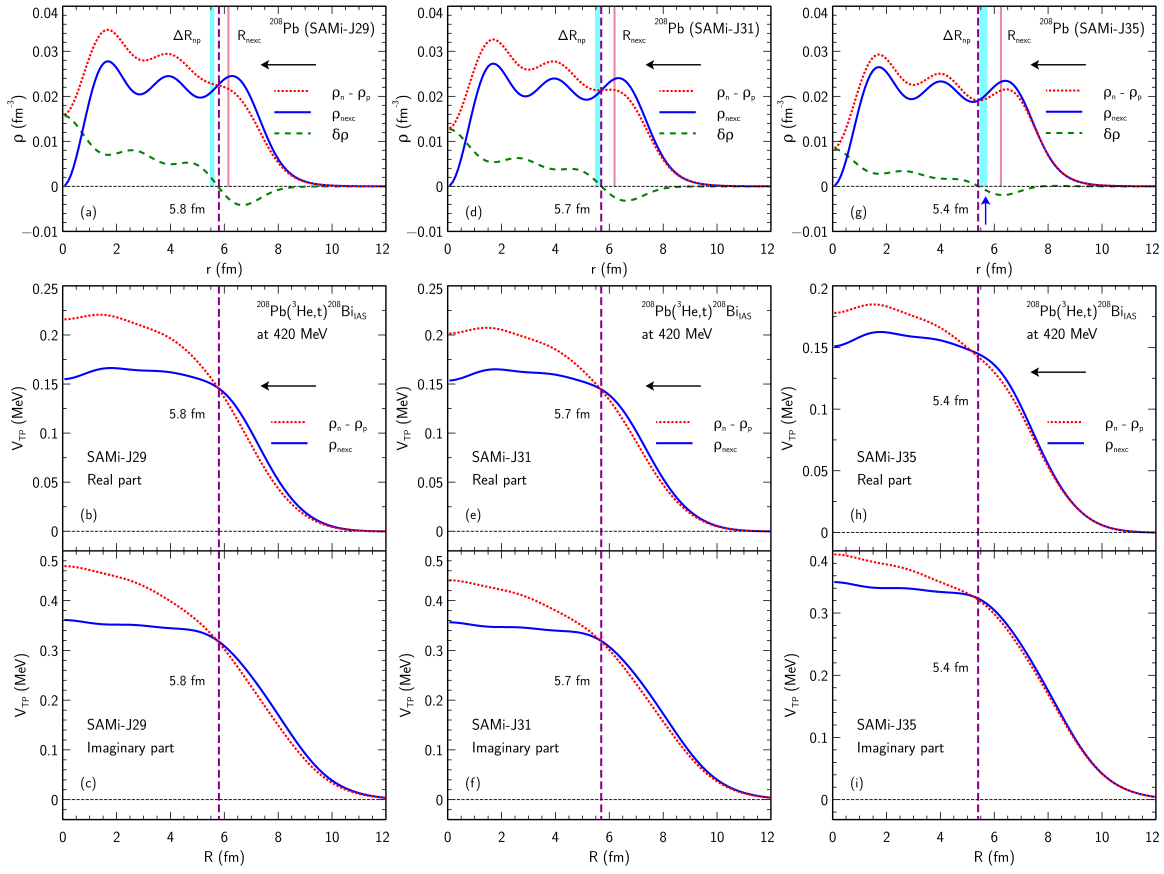


FIG. 2. Nuclear distributions of  $^{208}\text{Pb}$  for SAMi-J29, SAMi-J31, and SAMi-J35, illustrating isovector, neutron excess, and Coulomb core-polarization densities in (a, d, g). Real and imaginary parts of the transition potential using isovector and neutron excess densities are shown in (b, c) for SAMi-J29, (e, f) for SAMi-J31, and (h, i) for SAMi-J35. The divergence between neutron excess and isovector densities at the nuclear surface is featured. The neutron skin region is displayed by the cyan transparent area, and the rms neutron excess by the crimson transparent line. The direction of the incident particle probing the target is marked by black horizontal arrows, and the Coulomb boundary radius by purple dashed lines. The blue vertical arrow denotes where protons are mixed into the neutron skin area.

lies after the neutron skin region. This results in a mixed region where protons are driven into the neutron skin area (exhibited by a blue vertical arrow), causing neutron skin impurity due to the core-polarization influence. In this scenario, the incident particle first encounters the neutron excess, then probes an impurity neutron skin region where protons are mixed, introducing uncertainty in determining the exact neutron skin thickness if  $^{208}\text{Pb}$  is assumed to have a large neutron skin as suggested by the PREX-II results. This sequence implies that the incident particle initially probes the neutron excess, then reaches the Coulomb boundary, and finally probes the neutron skin if the neutron skin of  $^{208}\text{Pb}$  is consistent with the reanalyzed PREX-II and RCNP results, as seen in the case of SAMi-J29 and SAMi-J31.

The incident particle behavior, as previously discussed, is consistent if the neutron skin of  $^{208}\text{Pb}$  matches the reanalyzed PREX-II and RCNP results, as noted with SAMi-J29 and SAMi-J31. Our analysis centers on the

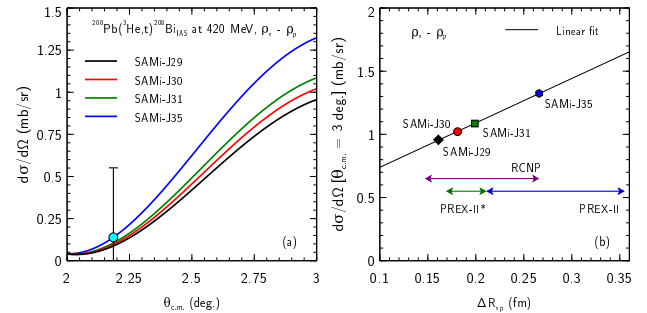


FIG. 3. (a) Differential cross section results of the  $(^3\text{He}, t)$  IAS reaction at scattering angles beyond the first minimum using SAMi-J interactions incorporating isovector density. (b) Linear correlation between the differential cross section at  $3^\circ$  and the neutron skin thickness for the same interactions. These results feature the sensitivity of the  $(^3\text{He}, t)$  IAS reaction to neutron skin thickness at  $3^\circ$ , where the core-polarization is negligible. Experimental data are from Zegers et al. [8].

scattering angle of  $3^\circ$ . Figure 3(a) presents the differential cross section from  $2^\circ$  to  $3^\circ$  using the same interactions as in Figure 1 and employing the isovector transition density. In this region, the core-polarization dynamics are insignificant, allowing the isovector density to determine the neutron skin thickness. As the neutron skin increases with different interactions, Figure 3(b) illustrates the differential cross section at  $3^\circ$  versus the neutron skin thickness. A linear trend similar to that in Figure 1(c) is observed, demonstrating that the  $(^3\text{He}, t)$ IAS reaction is sensitive to the neutron skin thickness at  $3^\circ$ , which is crucial for reliable determination.

It is vital to stress that the  $(^3\text{He}, t)$ IAS reaction probes the neutron excess at  $0^\circ$  due to the core-polarization process. However, once the incident particle traverses the Coulomb boundary, where this effect becomes negligible, it accurately probes the neutron skin. Therefore, the scattering angle of  $3^\circ$  is optimal for determining the precise neutron skin thickness in  $^{208}\text{Pb}$ . Theoretical models that fit well at scattering angles between  $2^\circ$  and  $3^\circ$  can correctly deduce the neutron skin thickness. We propose extending the  $(^3\text{He}, t)$ IAS experiment by Zegers et al. [8] at the Facility for Rare Isotope Beams (FRIB) to measure the differential cross section up to  $3^\circ$ , where the exact neutron skin thickness can be resolved without the interference of core-polarization. This method is practical and allows for direct comparison with PREX-II results. The advanced facilities at FRIB enable isobaric single charge-exchange reactions to be measured using exotic beams in inverse kinematics, allowing for measurements with minimal uncertainty.

- 
- \* [phannhuthuan@duytan.edu.vn](mailto:phannhuthuan@duytan.edu.vn)
- [1] F. Nunes, G. Potel, T. Poxon-Pearson, and J. Cizewski, *Annual Review of Nuclear and Particle Science* **70**, 147 (2020).
  - [2] B. Alex Brown, *Phys. Rev. Lett.* **85**, 5296 (2000).
  - [3] J. Zenihiro, H. Sakaguchi, T. Murakami, *et al.*, *Phys. Rev. C* **82**, 044611 (2010).
  - [4] S. Abrahamyan, Z. Ahmed, H. Albataineh, *et al.* (PREX Collaboration), *Phys. Rev. Lett.* **108**, 112502 (2012).
  - [5] D. Adhikari, H. Albataineh, D. Androic, *et al.* (PREX Collaboration), *Phys. Rev. Lett.* **126**, 172502 (2021).
  - [6] P.-G. Reinhard, X. Roca-Maza, and W. Nazarewicz, *Phys. Rev. Lett.* **127**, 232501 (2021).
  - [7] N. Auerbach and N. Van Giai, *Phys. Rev. C* **24**, 782 (1981).
  - [8] R. G. T. Zegers, T. Adachi, H. Akimune, *et al.*, *Phys. Rev. Lett.* **99**, 202501 (2007).
  - [9] B. M. Loc, D. T. Khoa, and R. G. T. Zegers, *Phys. Rev. C* **89**, 024317 (2014).
  - [10] P. N. Huan, N. L. Anh, B. M. Loc, and I. Vidaña, *Phys. Rev. C* **103**, 024601 (2021).
  - [11] B. M. Loc, N. Auerbach, and D. T. Khoa, *Phys. Rev. C* **96**, 014311 (2017).
  - [12] M. Toyokawa, M. Yahiro, T. Matsumoto, and M. Kohno, *Progress of Theoretical and Experimental Physics* **2018**, 023D03 (2018).
  - [13] E. Nielsen, D. Fedorov, A. Jensen, and E. Garrido, *Physics Reports* **347**, 373 (2001).
  - [14] Gianluca Colò and Ligang Cao and Nguyen Van Giai and Luigi Capelli, *Computer Physics Communications* **184**, 142 (2013).
  - [15] X. Roca-Maza, M. Brenna, B. K. Agrawal, *et al.*, *Phys. Rev. C* **87**, 034301 (2013).
  - [16] X. Roca-Maza, G. Colò, and H. Sagawa, *Phys. Rev. C* **86**, 031306 (2012).

# Supplemental Material for “Neutron skin impurity from Coulomb core-polarization in $^{208}\text{Pb}$ : Insights from PREX-II and validation via $(^3\text{He}, t)\text{IAS}$ reaction”

Phan Nhut Huan\*

*Institute of Fundamental and Applied Sciences, Duy Tan University, Ho Chi Minh City 70000, Vietnam and Faculty of Natural Sciences, Duy Tan University, Da Nang City 50000, Vietnam*

(Dated: May 30, 2024)

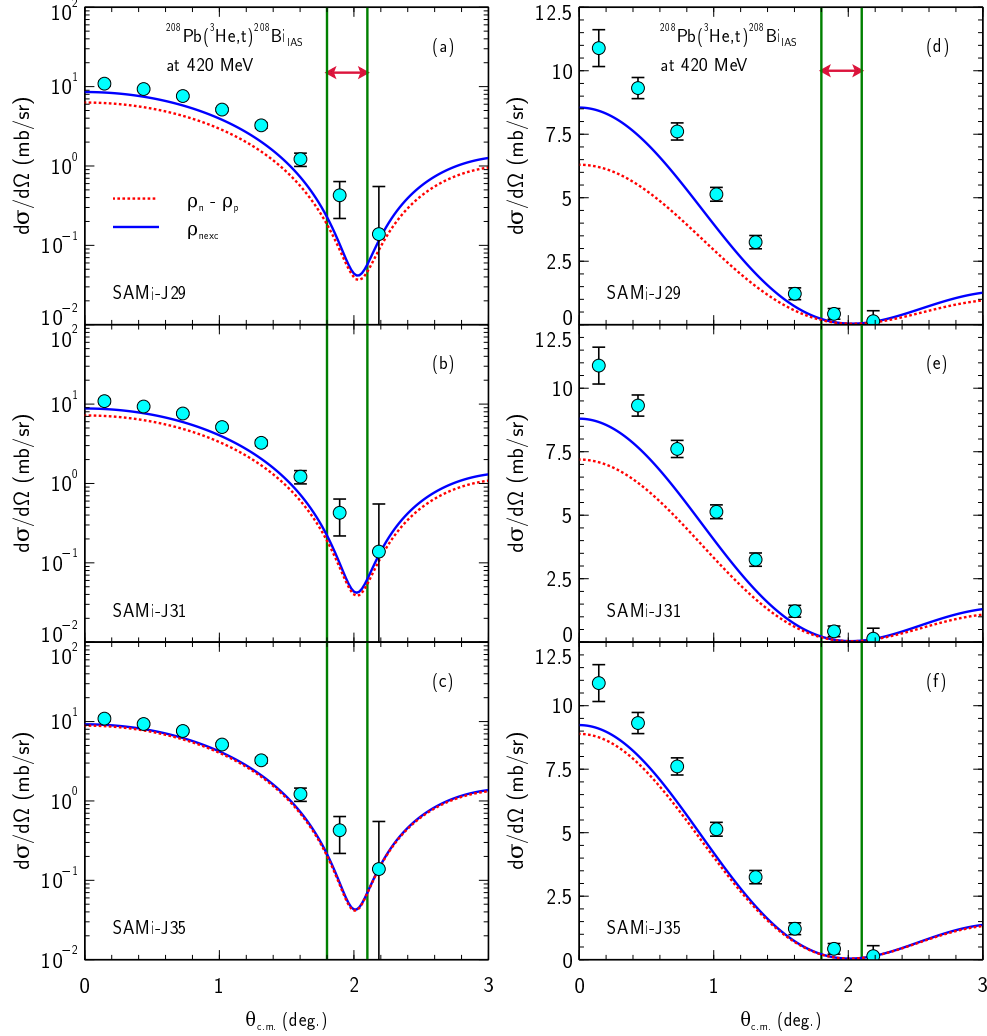


FIG. 1. Differential cross section of the  $(^3\text{He}, t)\text{IAS}$  reaction using isovector and neutron excess densities, presented in logarithmic scale (a, b, c) and linear scale (d, e, f) for different SAMi-J interactions: SAMi-J29 (a, d), SAMi-J31 (b, e), and SAMi-J35 (c, f). The crimson horizontal arrows indicate the region where the incident particle reaches the Coulomb boundary radius, with Coulomb core-polarization becoming negligible, approximately near the first minimum between  $1.8^\circ$  and  $2.1^\circ$ . Experimental data are from Zegers et al. [Phys. Rev. Lett. 99, 202501 (2007)].

## ACKNOWLEDGEMENTS

P. N. H. is grateful to Prof. Dao Tien Khoa for valuable support and discussions. He would also like to thank Dr. Bui Minh Loc for valuable suggestions and Prof. Nguyen Quang Hung for his support.